Green's function description of momentum-orientation relaxation of photoexcited electron plasmas in semiconductors

R. Binder
Optical Sciences Center, University of Arizona, Tucson, Arizona 85721

H. S. Köhler
Department of Physics, University of Arizona, Tucson, Arizona 85721

M. Bonitz
Optical Sciences Center, University of Arizona, Tucson, Arizona 85721

N. Kwong
Department of Physics, University of Arizona, Tucson, Arizona 85721

(Received 19 July 1996; revised manuscript received 23 September 1996)

We present numerical results for the momentum-orientation relaxation of optically excited electron plasmas in bulk semiconductors. Our results are based on the full two-time Green's function approach for carrier-carrier scattering and are compared to the results obtained within the conventional quantum Boltzmann equation. Defining ''memory effects'' by this comparison, we find memory effects mainly to be differences in the time-scale of the relaxation process rather than distinct qualitative features. Within the limitations of our isotropic static screening model, we find that, in both approaches, an initial anisotropic and nonmonotonic distribution function relaxes in a three-stage process in which the distribution becomes monotonic before it loses its anisotropy. [S0163-1829(97)11307-8]

I. INTRODUCTION

Optical excitation of electron-hole plasmas in semiconductors yields, in general, anisotropic momentum distributions of the excited charge carriers.[1–3] It is well known that even in bulk III-V semiconductors, such as GaAs, optical excitation creates anisotropic plasmas. This is mainly due to the specific optical transition matrix elements involving the heavy-hole (hh) and light-hole (lh) valence bands, respectively. A comprehensive discussion of the anisotropic aspects of optical excitation can be found in Ref. 4. This anisotropy will be the focus of this paper. Further contributions are due to the anisotropy of the effective mass (warping) which is discussed, for example, in Refs. 5 and 6, and, in the case of excitation very high into the interband continuum where intervalley scattering becomes important due to the strong cubic anisotropy related to the lattice structure of GaAs. This cubic anisotropy is also present in two-photon transition, in which higher lying conduction bands are involved.[7,8] In the following, we restrict ourselves to the anisotropy related to the optical transition matrix elements.

The initial anisotropy of the excited conduction band electrons results from the interplay between linear polarized light pulses and the specifics of the optical dipole matrix elements. It comprises two different contributions, one due to excitation from the heavy-hole valence band and one due to the light-hole valence band. The subsequent momentum orientation relaxation, i.e., the scattering processes that make the distribution of carriers essentially isotropic, is believed to be among the fastest scattering mechanisms in semiconductors and, in the high density regime, is dominated by carrier-carrier scattering.

Recently, the issue of so-called memory effects, i.e., the deviation of relaxation processes from simple Markov processes, has drawn considerable attention, e.g., Refs. 9–16. One might expect that such memory effects, if at all, should be most important in the fastest relaxation processes. For this reason, we present in this paper a study of memory effects in the momentum-orientation relaxation. The theoretical framework for charge-carrier relaxation is already well established. One of the most powerful techniques, which not only contains a proper description of memory effects but also includes incoherent carrier correlation effects self-consistently, is the nonequilibrium Green's function technique. This technique, which is based on the evolution of two-time correlation functions of one-particle expectation values, is usually used as a starting point in the derivation of the simpler equations-of-motion for one-time distribution functions (i.e., conventional Boltzmann scattering integrals, generalized Kadanoff-Baym equations, etc.). The investigation of relaxation processes in semiconductors based on the full two-time Kadanoff-Baym equations is still in an initial stage.[15–17] To the best of our knowledge, all previously reported two-time calculations addressing semiconductor properties are based on the additional assumption of isotropic distribution functions.

Whereas the main motivation of this study are effects which are formally beyond the Markov approximation, i.e., beyond the approximation in which the time-derivative of the carrier distribution at given time depends only on the distribution at that time, the most striking result to be discussed in the following is present even within the Markov approximation. It turns out that the system reaches isotropy in three stages. The initial fast orientation relaxation still

preserves the initial ellipsoidlike shape of the distribution function. It only evens out the distribution on the initial ellipsoidlike surface. Only on a distinctly slower time scale does the distribution become spherically isotropic (third stage). In between these two time scales is the relaxation that drives the distribution into a monotonically decaying function (i.e., monotonically decaying as a function of $|\vec{k}|$).

The theoretical basis of our analysis are the equations of motion for the the full two-time one-particle Green's function $g^{<}(\vec{k},t_1,t_2)$ within the screened-Hartree-Fock approximation. This Green's function reduces to the distribution function of the charge carriers as function of momentum $\vec{k}$ and time t in the equal time limit: $f(\vec{k},t)=-i\hbar g^{<}(\vec{k},t,t)$.

The most important advantage of the two-time Green's function approach is related to the fact that a self-consistent treatment of carrier kinetics (i.e., the temporal change of the distribution function) and carrier correlations (i.e., self-energy effects, damping, and ''dephasing'') is inherent to this approach. In many other theoretical approaches carrier correlation effects are accounted for by explicit energy renormalization of one-particle states, i.e., the renormalization of the one-particle electron energy $\varepsilon^{e}_{\vec{k}}$ by the complex self-energy $\Sigma^{e}_{\vec{k}}$. The strength of non-Markovian effects in the relaxation process is then crucially determined by the imaginary part of Σ, which is often referred to as damping or dephasing function. The requirement to treat kinetics and self-energy effects self-consistently often poses a difficult problem, which is completely avoided in the two-time Green's function approach. This is especially advantageous if the lead focus of the investigation is the prediction of the importance of memory effects.

Of course, from a practical point of view, there is still one significant disadvantage in the two-time Green's function approach: the numerical solution requires more cpu time. For this reason we restrict our investigations to the following situation. Instead of treating the optical excitation process dynamically, we solve only the initial value problem for the electron distribution. Also, we consider only electron-electron scattering and completely neglect the holes. Screening of the Coulomb potential is treated within a simple quasistatic model. Although the restriction to a one-band model makes a full simulation of the optical excitation and, more importantly, of the optical measurement process impossible, it still allows us to address the important and basic issue of non-Markovian relaxation characteristics in a high density plasma. This issue is independent of the specific optical pump-and-probe scenario. The understanding of the basic relaxation dynamics is actually a necessary prerequisite for the understanding of the more complex dynamical behavior of the coupled light-semiconductor system.

II. INITIAL DISTRIBUTION FUNCTION

In order to obtain a suitable initial distribution function for optically created conduction-band electrons, we follow Zakharchenya *et al.*[18] and use an angle dependence of the two electron components (one due to hh-c excitation and the other due to lh-c excitation) that results from perturbation theory of the optical excitation process with linearly polarized light. We denote the angle between a given momentum state $\vec{k}$ and the polarization vector of the light as θ. As shown in Ref. 18 the momentum dependent squared dipole matrix elements $|\langle c,\vec{k}|\vec{r}\cdot\vec{E}|v,\vec{k}\rangle|^2$ between the conduction band ''c'' and the valence band ''v,'' where v stands either for hh or lh denoting heavy-hole and light-hole, respectively, is proportional to $1\mp P_2(\cos\theta)$, where ''$-$'' gives the contribution due to the hh-c transition and ''$+$'' that of the lh-c transition. P_2 is the second degree Legendre polynomial. Not given in Ref. 18 are the proportionality factors which depend only on the modulus of $\vec{k}$ and the details of the optical excitation such as the amplitude, duration, and center-frequency of the optical excitation field $\vec{E}$. In the following analysis we proceed quasiphenomenologically and use prefactors which correspond to an optical excitation process in which the distribution function reflects the spectral shape of the optical pulse which we take to be Gaussian. In the context of a third-order approximation of the semiconductor Bloch equations without Coulomb interaction this can be achieved in an approximate way, if, in the time derivative of the distribution function, the interband polarization function is always taken at times long after the pulse. This procedure yields Gaussian distribution functions centered at the carrier momentum that corresponds to the resonance condition of the excitation field: $\hbar\omega_0=\varepsilon^{e}_{k}+\varepsilon^{a}_{k}$ with $a=$hh,lh. Here, ω_0 is the center frequency of the light pulse, $\varepsilon^{e}_{\vec{k}}=\hbar^2k^2/2m_e+E_G$ is the electron energy with effective mass m_e, E_G is the band-gap energy, $\varepsilon^{\mathrm{hh}}_{\vec{k}}=(\hbar^2k^2/2m_0)(\gamma_1-2\gamma_2)$ is the heavy-hole energy with Luttinger parameters γ_1 and γ_2 (m_0 is the electron mass in vacuum), and $\varepsilon^{\mathrm{lh}}_{\vec{k}}=(\hbar^2k^2/2m_0)(\gamma_1+2\gamma_2)$ is the light-hole energy. Our initial distribution therefore contains two contributions with slightly different center-momenta (due to the mass difference of hh and lh) and different angle characteristics (because the hh has an angular momentum quantum number of $j=\pm 3/2$ with respect to the quantization axis given by $\vec{k}$, whereas the lh has $j=\pm 1/2$):

$$f(\vec{k},0)=\mathcal{A}_{\mathrm{hh}}(k)\frac{1}{2}[1-\cos^2\theta]+\mathcal{A}_{\mathrm{lh}}(k)\frac{1}{6}[1+3\cos^2\theta], \tag{1}$$

with

$$\mathcal{A}_a(k)=A_0\exp(-(\hbar\omega_0-\varepsilon^{e}_{k}-\varepsilon^{a}_{k})^2/(2\gamma^2)), \tag{2}$$

where $A_0=(\mu_0\mathcal{E}_0)^2\pi/2\gamma^2$, μ_0 is the angle-independent part of the interband dipole moment, $\mathcal{E}_0$ is the peak light-field amplitude, and the width of the distribution is related to the pulse duration τ (FWHM of intensity) through $\gamma^2=\hbar^2 2\ln 2/\tau^2$. This appoach, in which the light-field parameters enter only into the shape of the initial distribution, is strictly justified only if the relaxation processes are much slower than the light-pulse duration τ.

III. THEORETICAL APPROACHES

The temporal evolution of the one-particle Green's functions $g^{\gtrless}(\vec{k},t,t')$ is determined by the Kadanoff-Baym equations (for a derivation see, for example, Ref. 19)

$$\left(i\hbar\frac{\partial}{\partial t}-\varepsilon^{e}_{\vec{k}}\right)g^{\gtrless}(\vec{k},t,t') = \int_{t_0}^{t} d\overline{t}\{\Sigma^{>}(\vec{k},t,\overline{t})-\Sigma^{<}(\vec{k},t,\overline{t})\}g^{\gtrless}(\vec{k},\overline{t},t') - \int_{t_0}^{t} d\overline{t}\,\Sigma^{\gtrless}(\vec{k},t,\overline{t})\{g^{>}(\vec{k},\overline{t},t')-g^{<}(\vec{k},\overline{t},t')\}. \quad (3)$$

Within the screened-Hartree-Fock approximation and the additional approximation of quasistatic screening, the self-energy $\Sigma^{\gtrless}(\vec{k},t,t')$ is given by

$$\Sigma^{\gtrless}(\vec{k},t,t') = \sum_{\vec{k}',\vec{q}} 2W(q,t)W(q,t')g^{\gtrless}(\vec{k}+\vec{q},t,t') \times g^{\gtrless}(\vec{k}'-\vec{q},t,t')g^{\gtrless}(\vec{k}',t',t), \quad (4)$$

where $W(q,t)=4\pi e^2/[q^2+\kappa^2(t)]$ is the quasistatically screened Coulomb potential in Gauss units. Here, $e^2=e_0^2/\epsilon_b$ is the effective charge squared (e_0 is the electron charge in vacuum and ϵ_b is the background dielectric constant of the semiconductor) and κ is the screening wave number. As for the initial condition, we assume that at the initial time t_0 all correlations vanish and that the equal-time Green's function $-i\hbar g^{<}(\vec{k},t_0,t_0)$ is the initial distribution discussed above. Due to the specific retardation described by Eqs. (3) and (4) the initial condition at a single point in the t-t' plane is sufficient to obtain the solution for all $t,t'>t_0$.

The static screening approximation is a significant restriction concerning the quantitative reliability of the theoretical model. The importance of dynamical screening models was pointed out, for example, in Ref. 20 and it was shown (see, for example, Ref. 21) that for Markovian Boltzmann equations the static screening model yields smaller scattering rates than dynamic screening models (in this case the Boltzmann equation is known as the Lenard-Balescu equation). Since, for the time being, a general two-time screened potential within the two-time Green's function formalism is not feasible, we solve the Kadanoff-Baym equations twice: once with a screening wave number that underestimates the screening and once with one that overestimates the screening. For the interpretation of our results we consider only those features that are common to both results.

In order to interpret the results based on the two-time formalism and to extract features which could be ascribed to memory effects, we compare and contrast that theoretical approach with the conventional Boltzmann equation. There are several ways to obtain the conventional Boltzmann equation from the two-time formalism (see, for example, Refs. 19 and 22). The principle characteristic of non-Markovian relaxation equations is, of course, the dependence of the time derivative of the distribution function, $\dot{f}(t)$, on the distribution function $f(t')$ at earlier times $t'<t$. In the Markov approximation, the scattering integral determining $\dot{f}(t)$ depends only on $f(t)$. There exist, however, many different versions of Markovian scattering integrals. The differences between the various Markovian scattering integrals are related to different screening functions and different one-particle self-energies. In the simplest version, the one-particle self-energies are neglected and, in particular, do not contain imaginary parts (damping or dephasing constants). In that limit, and under the additional assumption of large times (i.e., $\hbar/[t-t_0]\ll$ typical energy transfers), the kinetic energy becomes a constant of motion (i.e., the scattering integral contains a kinetic energy conserving δ function). In a recent study[15] we have investigated carrier relaxation in isotropic plasmas and compared various approximation schemes. In the following we will restrict ourselves to the comparison of the two-time Kadanoff-Baym equations with the simplest conventional Boltzmann equation,

$$\frac{\partial}{\partial t}f(\vec{k},t)=\Gamma_{\rm in}[f;\vec{k},t][1-f(\vec{k},t)]-\Gamma_{\rm out}[f;\vec{k},t]f(\vec{k},t), \quad (5)$$

where $\Gamma_{\rm in}$ is the in-scattering rate,

$$\Gamma_{\rm in}[f;\vec{k},t]=\frac{2\pi}{\hbar}\sum_{\vec{k}',\vec{q}} 2|W(q,t)|^2 f(\vec{k}+\vec{q},t)f(\vec{k}'-\vec{q},t) \times[1-f(\vec{k}',t)] \times\delta(\varepsilon_{\vec{k}}+\varepsilon_{\vec{k}'}-\varepsilon_{\vec{k}+\vec{q}}-\varepsilon_{\vec{k}'-\vec{q}}) \quad (6)$$

and $\Gamma_{\rm out}$ is the out-scattering rate which can be obtained from $\Gamma_{\rm in}$ by replacing f by $1-f$.

The numerical procedures for solving both the Kadanoff-Baym equations and the conventional Boltzmann equation are the same as used in Ref. 16. That reference also contains a discussion of the more technical aspects of modifying an algorithm for solving the Kadanoff-Baym equations to also solve the conventional Boltzmann equation [see Eq. (2.16) of Ref. 16].

IV. RESULTS AND DISCUSSION

For the numerical evaluations we chose material parameters appropriate for GaAs: the effective electron mass is $m_e=0.067m_0$, and the excitonic Rydberg energy is $E_R=4.2$ meV, correponding to a background dielectric constant $\epsilon_b=12.998$ and an exciton Bohr radius $a_B=132$ Å. The Luttinger parameters are $\gamma_1=6.85$ and $\gamma_2=2.1$. The light-pulse polarization is chosen to be in the z-direction. The initial conditions are $\hbar\omega_0=E_G+50$ meV, $\tau=40$ fs, and $A=1.2$. The electron density is 6.1×10^{17} cm^{-3}. The maximum k-value (in each Cartesian direction) was chosen to be between 6.3 and 8.7 in units of a_B^{-1} and the number of k points in each direction was between 43 and 59. Within this parameter range, the results were found to be insensitive to the parameters.

In the following we present contour plots for the distribution function at $k_y=0$. The distribution for $k_y\neq0$ can be obtained from the results shown by rotating them around the z axis.

Figure 1 shows the initial electron distribution which consists of the two components from the hh and lh transitions shown separately in Figs. 2 and 3. The initial distribution differs from a quasiequilibrium distribution, to which it relaxes by means of c-c scattering, in three aspects: (i) in radial direction, the function is nonmonotonic, due to carrier

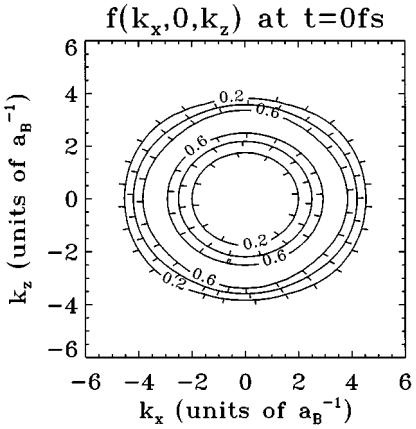

FIG. 1. Initial charge-carrier distribution of conduction band electrons excited from the heavy-hole and light-hole bands as a function of momentum vector $\vec{k}$. The distribution is shown for $k_y=0$. The distribution in three-dimensional momentum space is obtained from this figure by rotation about the z axis. The units of the wave numbers k_x and k_z in this and all other contour plots are inverse Bohr radii (a_B^{-1}). The parameters are given in the text. The contour lines show equally spaced levels with the value of the distribution indicated on selected contour lines. The tick marks on the contour lines point in the ''down-hill'' direction.

excitation high in the band; (ii) due to the mass (or, equivalently, density-of-states) difference between the heavy- and the light-hole band, the location of the distribution maximum depends on the direction of $\vec{k}$ (peak in k_x direction from heavy-hole contribution, peak in k_z direction from light-hole contribution); (iii) also due to the mass difference, the height of the maximum distribution is anisotropic.

If, instead of a quasiphenomenological initial condition we would fully simulate the optical excitation process, we should still expect these three qualitative features. The quantitative details might, of course, differ from our model. Also different from our model would be the fact that during the optical excitation charge-carrier correlations build up. Our model of vanishing initial correlations is likely to underestimate the speed of initial scattering processes since in a theoretical model containing memory effects the time derivative $\dot{f}$ is zero at $t=t_0$. This point is discussed in more detail in Ref. 15.

We will present two different sets of results: one for a

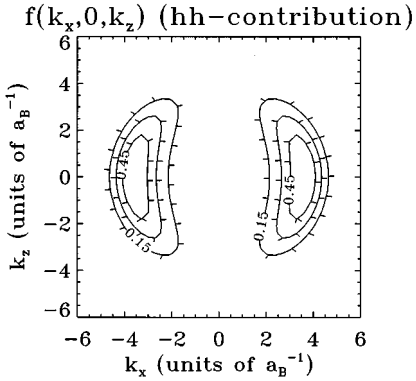

FIG. 2. The contribution to Fig. 1 from the heavy-hole (hh) band excitation.

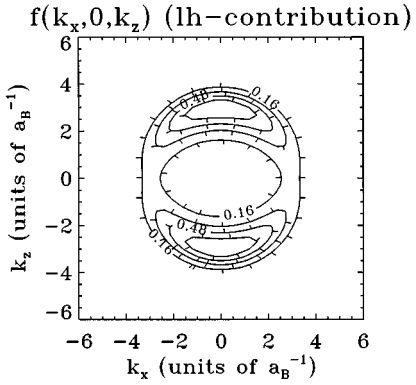

FIG. 3. The contribution to Fig. 1 from the light-hole (lh) band excitation.

weakly screened potential and one for a strongly screened potential. In the case of the strongly screened potential we choose the (time-dependent) screening wave number to correspond to the full density, $\kappa^2(t)=(4e^2m_e/\pi\hbar^2)\int_0^\infty dk f(k,t)$, where $f(k,t)$ is the angle-averaged distribution. In other words, $\kappa(t)$ is computed self-consistently with the time-dependent distribution functions. The value of κ for our parameters is between $1.5a_B^{-1}$ (initially) and $1.8a_B^{-1}$ at $t=160$ fs. Because of the nonzero build-up time of static screening this is likely to overestimate the screening. Therefore we investigate also the relaxation in the limit of a weakly screened potential, where we chose a constant $\kappa=0.4a_B^{-1}$. This is, of course, an arbitrary choice, but it is still reasonable to believe that the results for the weakly screening potential are more realistic than those obtained with the self-consistent $\kappa(t)$.

We begin the discussion of the time evolution of the distribution function on the basis of the two-time Kadanoff-Baym equations with a weakly screened potential. Figures 4 and 5 show that the fastest process is the relaxation toward a quasi-isotropic distribution, i.e., a distribution in which the different peak heights in the k_x and k_y direction, respectively, are evened out, but the oval shape of the distribution still persists (Fig. 4). It is followed by the relaxation toward a

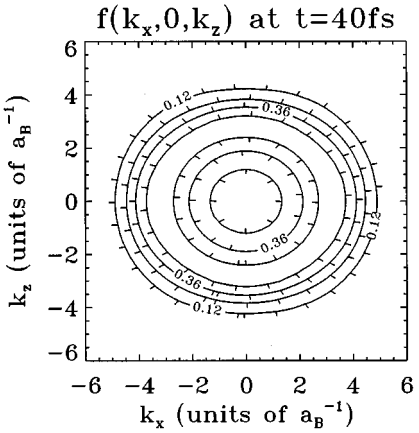

FIG. 4. Relaxation of electron distribution (sum of hh+lh contributions) calculated with the two-time Kadanoff-Baym equations with a strong interaction potential ($\kappa=0.4a_B^{-1}$). The other parameters are given in the text. The time is 40 fs.

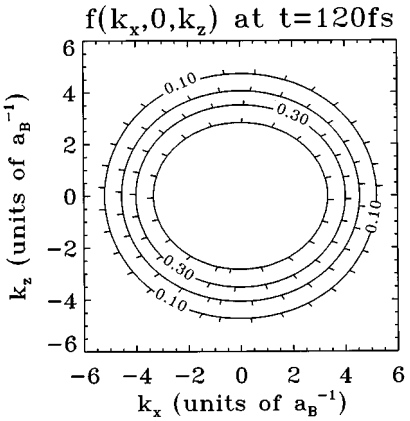

FIG. 5. Same as Fig. 4, but for time $t=120$ fs.

completely monotonically decreasing function in all directions which, however, is still not spherically isotropic (Fig. 5). During the final and third stage, the oval and monotonic distribution will eventually become a spherically isotropic and monotonic quasiequilibrium function. This function will be essentially a Fermi function, except for the minor modifications due to charge-carrier correlations built up during the relaxation process.

To compare these results with the case of a strongly screened Coulomb potential, in which the relaxation rates are likely to be underestimated, we show in Fig. 6 the distribution at $t=120$ fs. As expected, the relaxation is now much slower, but other than that no qualitative differences appear (instead of proving this statement by showing more contour plots, we will come back to this point in the discussion of the quadrupole moments below).

One of the goals of this investigation is the identification of memory effects. To this end we have solved the conventional Boltzmann equation. In Figs. 7 and 8 we see that conventional Boltzmann relaxation is faster than the one computed with the full two-time formalism (compare Figs. 4 and 5). The main reason is, similar to the case of isotropic relaxation, the presence of initial nonzero relaxation rates and conservation of kinetic energy in the conventional Boltzmann equation. These differences are most pronounced at early times (see the results for 40 fs). Other than the quantitative difference regarding the speed of the relaxation, we have not found any strong and qualitative memory effects. This, again, agrees with our findings for the isotropic relaxation,[15] where qualitative memory effects were obtained only within the so-called ''free generalized Kadanoff-Baym ansatz,'' an approximation which completely neglects damping effects. Figure 8 also shows that the relaxation tends indeed towards a spherical isotropic final distribution. As for the fast initial relaxation dynamics illustrated in Fig. 7, we see that the nonequilibrium peak of the hh contribution has broadened more than that of the lh contribution which, in the figure, leads to an almost circular shape of the inner circle representing the low-momentum boundary of the nonequilibrium distribution. The faster hh relaxation can be attributed to the larger density of the hh contribution. Although the maximun occupation is higher, by a factor 4/3, for the lh contribution than for the hh contribution [see Eq. (1)], the initial hh-contribution density contains more charge carriers. This is due to the larger joint density-of-states of the hh-to-conduction-band transition compared to that of the light holes. Since, within our model, the joint density-of-states is proportional to $m_{\mathrm{red},a}^{3/2}$ (where $a=$hh,lh and the inverse reduced mass is $m_{\mathrm{red},a}^{-1}=m_e^{-1}+m_a^{-1}$), the density of the hh contribution is larger, by a factor of 1.79, compared to that of the light holes. Of course, there is no strict separation in terms of scattering within the hh contribution versus scatter-

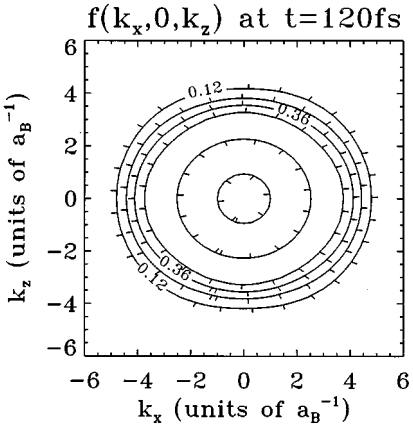

FIG. 6. Same as Fig. 5, but calculated with a weak interaction potential [self-consistent $\kappa(t)$].

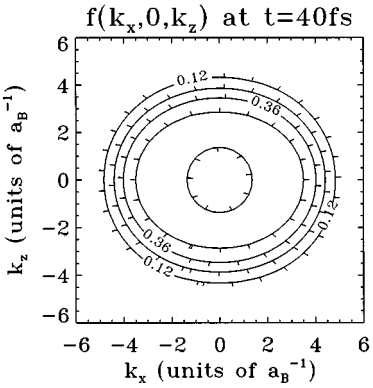

FIG. 7. Relaxation of electron distribution (sum of hh+lh contributions) calculated with the anisotropic single time Boltzmann equation with a strong interaction potential ($\kappa=0.4a_B^{-1}$). The time is 40 fs.

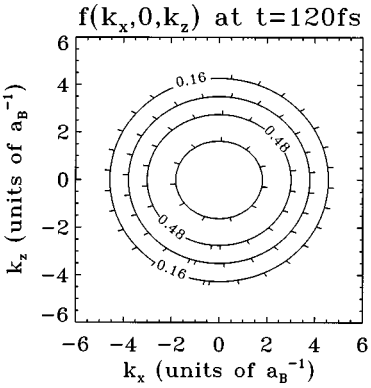

FIG. 8. Same as Fig. 7, but for time $t=120$ fs.

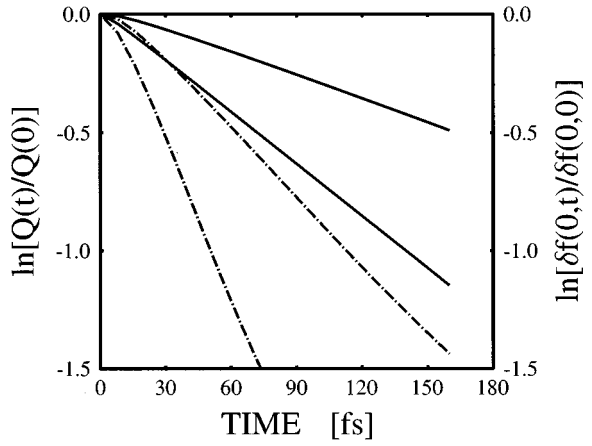

FIG. 9. Logarithm of the quadrupole moment $Q(t)$ (solid curves) and distribution difference at zero momentum $\delta f(0,t)$ (dash-dotted curves) for the case of the strong interaction potential. The distribution difference is defined as $\delta f(0,t)=f(0,t)-f(0,\infty)$. Shown are results computed with the two-time Kadanoff-Baym equations (upper solid and upper dash-dotted curve) and the single-time Boltzmann equation (lower solid and lower dash-dotted curve).

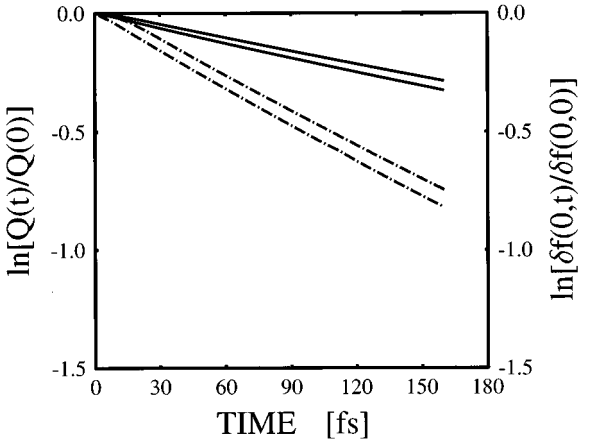

FIG. 10. Same as Fig. 9, but for the weak interaction potential.

ing within the lh contribution, but to the extent that small-momentum transfer scattering processes dominate the relaxation this concept is applicable at least in an approximate way.

For the case of the weak interaction potential, the relaxation process without memory is similar to that with memory and, therefore, leads to a similar contour plot (not shown). The absence of any clear memory effects in this case is not unexpected, because we found this in our earlier study of isotropic relaxation.[15]

Although we do not believe it to be very likely, we presently cannot rule out that the full inclusion of nonequilibrium plasmon and screening dynamics[10,12,23] would yield more pronounced memory effects in the orientation relaxation process.

To further analyze the relaxation processes and, in particular, to address the question whether the loss of anisotropy or the loss of nonmonotonicity is faster, we present in Figs. 9 and 10 the quadrupole moment of the distribution and the distribution at $\vec{k}=0$ in logarithmic form as a function of time. The quadrupole moment is defined as

$$Q(t)=\sum_{\vec{k}} Y_0^2(\theta,\phi) f(\vec{k},t), \tag{7}$$

where Y_0^2 is the spherical harmonic, θ is the polar angle, and ϕ is the azimuth angle of $\vec{k}$. Contrary to our earlier expectation, the numerical results show that the loss of anisotropy is slower than what is sometimes called ''energy relaxation,'' i.e., the scattering process in which the individual carriers (but not the total charge carrier system) change their kinetic energy. To extract an exponential decay rate from these figures one has to read off the time at which the logarithm drops to -1.

One can also compare the results shown so far with data obtained within a fully isotropic model. To this end we use the angle-averaged initial distribution

$$\overline{f}(k,0)=[\mathcal{A}_{\rm hh}(k)+\mathcal{A}_{\rm lh}(k)]/3. \tag{8}$$

We have solved the corresponding fully isotropic Boltzmann equation for $\kappa=0.4a_B^{-1}$ (strong potential) in order to compare this case with the anisotropic case shown in Figs. 7 and 8 and Fig. 9. The distribution for the fully isotropic case is shown in Fig. 11. The comparison shows that, if one is only interested in the overall relaxation speed and not in the details of the anisotropic character of the distribution, the isotropic calculation is sufficient because it yields very good agreement with the relaxation time found in the anisotropic case. The temporal behavior of the logarithm of the distribution at $k=0$ is almost identical to the corresponding result of Fig. 9.

Although there exist experimental investigations of momentum orientation relaxation in GaAs, we believe that the details of the three-stage process of electron relaxation discussed above has not been observed. The pioneering experiment of Oudar *et al.*[1] was performed at a time when tempo-

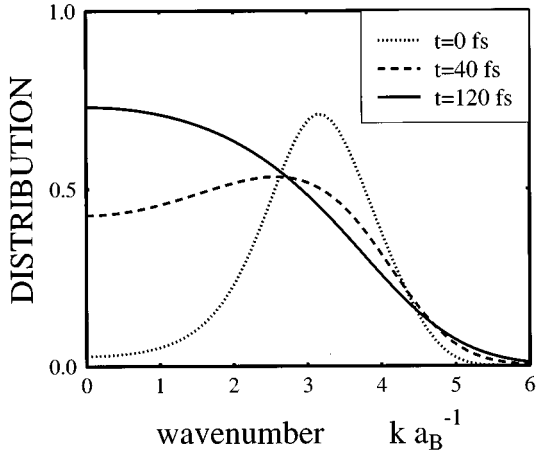

FIG. 11. Distribution function at various times for the fully isotropic case calculated with the single-time Boltzmann equation with the strong interaction potential.

ral resolution of ultrashort pulses was still in the 100 fs regime. Portella *et al.*[2] were able to use 9 fs pulses, but did not discuss the relative speed of orientation vs one-particle energy relaxation. It should also be noted that the measured optically induced dichroism and birefringence is a complicated function of the two theoretically observed anisotropy aspects, namely the anisotropic peak height and the oval shape, respectively, and also depends on how the nonmonotonicity affects the measurement of the anisotropy. A full microscopic theory for the specific experimental measurement process would be needed to identify these aspects in the measured signal. This applies in particular to the issue of memory effects, which, within the isotropic static screening approximation, and based on a fully self-consistent relaxation approach with damping, we have found to be only of quantitative rather than qualitative nature.

In summary, we have discussed various aspects of electron-electron scattering induced relaxation processes in optically created non-equilibrium electron plasmas in GaAs. We have found that the anisotropy decays slower than the non-monotonicity. The details depend on the exact form of the interaction potential. Furthermore, we have found memory effects to be appreciable only in the case of a strong (i.e., weakly screened) potential.

Note added. A related study of carrier-carrier scattering in semiconductors utilizing the two-time formalism for isotropic distributions has been published by W. Schäfer [J. Opt. Soc. Am. B **13**, 1291 (1996)].

ACKNOWLEDGMENTS

This work is supported by grants from JSOP, NSF, COEDIP (University of Arizona), DFG (Germany), DAAD (Germany), and grants for CPU time at CCIT, University of Arizona, and HLRZ Jülich (Germany).

[1] J. L. Oudar, A. Migus, D. Hulin, G. Grillon, J. Etchepare, and A. Antonetti, Phys. Rev. Lett. **53**, 384 (1984).
[2] M. Portella, J. Y. Bigot, R. W. Schoenlein, J. E. Cunningham, and C. V. Shank, Appl. Phys. Lett. **60**, 2123 (1992).
[3] M. A. Osman and N. Nintunze, in *Proceedings of the SPIE—The International Society for Optical Engineering* (The International Society for Optical Engineering, Bellingham, WA, 1994), Vol. 2142, pp. 207–277.
[4] *Optical Orientation*, edited by F. Meier and B. Zakharchenya (North-Holland, Amsterdam, 1984).
[5] J. A. Kash, M. Zachau, M. A. Tischler, and U. Ekenberg, Phys. Rev. Lett. **69**, 2260 (1992).
[6] M. Dür, K. Unterrainer, and E. Gornik, Phys. Rev. B **49**, 13 991 (1994).
[7] D. Dvorak, W. A. Schroeder, D. R. Andersen, A. L. Smirl, and B. S. Wherrett, IEEE J. Quantum Electron. **30**, 256 (1994).
[8] D. C. Hutchings and B. S. Wherrett, Phys. Rev. B **52**, 8250 (1995).
[9] A. V. Kuznetsov, Phys. Rev. B **44**, 8721 (1991).
[10] H. Haug and C. Ell, Phys. Rev. B **46**, 2126 (1992).
[11] D. TranThoai and H. Haug, Z. Phys. B **91**, 199 (1993).
[12] K. El Sayed, S. Schuster, H. Haug, F. Herzel, and K. Henneberger, Phys. Rev. B **49**, 7337 (1994).
[13] J. Schilp, T. Kuhn, and G. Mahler, Phys. Rev. B **50**, 5435 (1994).
[14] L. Banyai, D. B. T. Thoai, E. Reitsamer, H. Haug, D. Steinbach, M. U. Wehner, M. Wegener, T. Marschner, and W. Stolz, Phys. Rev. Lett. **75**, 2188 (1995).
[15] M. Bonitz, D. Kremp, D. Scott, R. Binder, W. Kraeft, and H. Köhler, J. Phys. Condens. Matter **8**, 6057 (1996).
[16] H. S. Köhler, Phys. Rev. E **53**, 3145 (1996).
[17] M. Hartmann and W. Schäfer, Phys. Status Solidi B **173**, 165 (1992).
[18] B. P. Zakharchenya, D. N. Mirlin, V. I. Perel, and I. I. Reshina, Usp. Fiz. Nauk **136**, 459 (1982) [Sov. Phys. Usp. **25**, 143 (1982)].
[19] L. P. Kadanoff and G. Baym, *Quantum Statistical Mechanics* (Addison-Wesley, New York, 1989).
[20] P. Lugli and D. K. Ferry, Phys. Rev. Lett. **56**, 1295 (1986).
[21] R. Binder, D. Scott, A. E. Paul, M. Lindberg, K. Henneberger, and S. W. Koch, Phys. Rev. B **45**, 1107 (1992).
[22] R. Binder and S. Koch, Prog. Quantum Electron. **19**, 307 (1995).
[23] G. Manzke, K. Henneberger, J. Heeg, K. El Sayed, S. Schuster, and H. Haug, Phys. Status Solidi B **188**, 395 (1995).